

Structural interpretation of the Tuzgolu and Haymana Basins, Central Anatolia, Turkey, using seismic, gravity and aeromagnetic data

Attila Aydemir¹ and Abdullah Ates²

¹Turkiye Petrolleri A. O. Mustafa Kemal Mah. 2. Cad. No: 86, 06520 Sogutozu, Ankara, Turkey

²Ankara University, Faculty of Engineering, Department of Geophysical Engineering, 06100, Besevler, Ankara, Turkey

(Received August 29, 2005; Revised February 21, 2006; Accepted May 12, 2006; Online published September 16, 2006)

The Tuzgolu Basin is the largest basin in Central Anatolia. It is connected to the Haymana Basin by a small channel-shaped basin called the Tersakan Basin. The study area has smooth topography with a stable young sedimentary cover and limited outcrop zones, but displays a complex geology with intense active tectonism and poor seismic quality beneath the surface. In the study reported here an attempt was made to determine the subsurface structure of the basement by three-dimensional modelling of gravity data. The seismic and magnetic data were also integrated with the available geological data to check the modelling results. The modelling results suggest that the deeper parts of the Haymana Basin are located to the east of Haymana city centre, at a maximum depth of 8 km, with the exception of the depression to the north, which is located 25 km northwest of Bala city centre at a maximum depth of 10 km. The channel-shaped Tersakan Basin (connecting the Haymana and Tuzgolu Basins) is located west of Lake Tuzgolu, and the deepest part of this basin is approximately 5.5 km. The Tuzgolu Basin has three major depressions: (1) the Southern Aksaray Depression, which is covered by younger volcanic rocks, is the largest but in general the least explored area; (2) the Eregli Depression; (3) the Sultanhanı Depression. Almost all of these depressions have an average depth of 8 km; however, some of the deeper segments are at a depth of approximately 12–13 km. Our results suggest the possibility of hydrocarbon potential in these basins.

Key words: Tuzgolu, Haymana, Tersakan Basins, Southern Tuzgolu High, Southern Aksaray Depression, three-dimensional modelling.

1. Introduction

The Tuzgolu Basin is located in Central Anatolia, Turkey. It is connected to the Haymana Basin to the north by means of a small channel-shaped basin called Tersakan Basin and, taken on a whole, all such basins can be considered collectively as Central Anatolian Basins. These basins are located the south of Ankara and extend down to the Taurus Mountains. Some of the more important towns in the study area are Kirsehir, and Aksaray to the east and Polatli and Konya to the west. The sedimentology and stratigraphy of these basins have been intensively studied using surface geology with limited outcrop data (Rigo de Righi and Cortesini, 1959; Unalan *et al.*, 1976; Gorur and Derman, 1978; Derman, 1979; Dincer, 1978; Dellaloglu and Aksu, 1984; Dellaloglu, 1991; Gorur *et al.*, 1998; Cemen *et al.*, 1999). Many authors have pointed out the importance of these basins and estimated the approximate thicknesses of sedimentary units by measuring the apparent thicknesses at outcrops. In previous analytical studies on the development of the basin, insufficient attention was given to the geophysical data when attempting to determine sedimentary thickness and the evolution of the area. Only a few papers—Ugurtas (1975), Ates and Kearey (2000) and Aydemir and Ates (2005)—utilized a limited geophysical data

set in their study. Aydemir and Ates (2005) produced upward continued gravity and aeromagnetic data in order to determine deeper zones in the basins that accommodated thick sedimentary deposition and deeper anomalous masses controlling the sedimentation. Some of the buried structural components that produced evident anomalies were studied by Kadioglu *et al.* (1998), Ates (1999). Gravity and aeromagnetic anomalies to the south of Konya were also studied by Ates and Kearey (2000). However, these studies were performed using aeromagnetic and gravity data, generally on small and local anomalies.

Despite a stable surface geology, the basins in the study area have a complex geology with strong active tectonism; they are also characterised by poor seismic quality beneath the surface. In addition, salt-bearing formations, including diapires and other salt structures, make seismic methods difficult, even rendering them incapable of evaluating the basin development and geometry.

In this paper, we have integrated all of the available geological and geophysical data, such as seismic, gravity, aeromagnetic and borehole data, in order to obtain accurate results by which to determine the basement geometries and main structural characteristics of the Tuzgolu and neighbouring basins. Three-dimensional (3-D) gravity interpretations were constructed with data obtained from the seismic sections and boreholes.

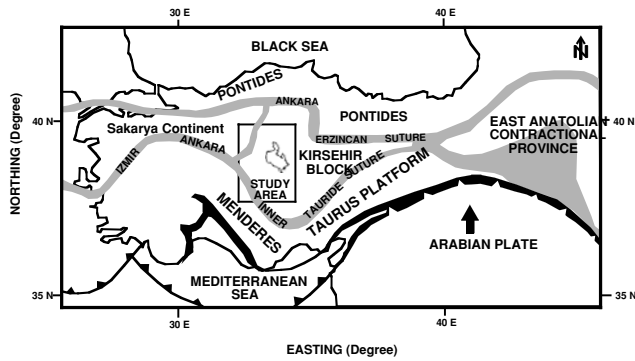


Fig. 1. Tectonic map of the study area. Modified from Gursöy *et al.* (1998)

2. Geological Setting

The study area is located to the south of the Izmir-Ankara-Erzincan and to the east of the Inner Tauride sutures, respectively (Fig. 1). Its location can also be described as being situated in the Kırşehir Block. Both suture zones are remnants of northern and southern branches of the Neo-Tethys Ocean. McClusky *et al.* (2000) suggested an anticlockwise rotation of Anatolia in association with a westward movement. The Kırşehir Block was also rotated in the same direction from the Cretaceous time (Sanver and Ponat, 1981). The neighbouring Menderes-Taurus Platform (Sengör and Yılmaz, 1981) to the west and south and the Kırşehir Block are both composed of metamorphic basements that include remnants of ophiolites derived from the northern branch of Neo-Tethys. Although the research area is surrounded by two important suture zones, the only major tectonic unit on the surface is the right lateral Sereflikochisar-Aksaray Fault that extends from N-NW to the S-SE direction, almost at the eastern boundary of the Tuzgolu Basin (Fig. 2). The plutonic intrusions, which originated from the subduction of the northern branches of the Neo-Tethys Ocean, can be observed to the east of the Sereflikochisar-Aksaray Fault and past the eastern boundary of the Tuzgolu Basin.

A generalised surface geological map of the study area is given in Fig. 2. Most of the surface is covered by young sediments (mostly Tertiary in age) surrounded by units of Sakarya Continent and two important metamorphic massives—the Kırşehir Metamorphics to the east and the Kutahya-Bolkardagi Metamorphics, which originated from the Menderes-Taurus Platform, to the west. The outcrops of ophiolitic, mafic-ultramafic rocks of previous oceanic crusts can also be observed in very limited zones. Additionally, terrestrial volcanic rocks (i.e. Calis, Karacadag and Deliler volcanites), which resulted from the tectonic movements that occurred at different times throughout the geological history, are outcropped in limited areas and are also encountered as intercalations with sedimentary deposits. The age (Late Cretaceous, Mid-Late Eocene and Late Miocene-Quaternary) of these volcanic rocks is identical to the main tectonic periods in the Central Anatolia (Dincer, 1978; Dellalolu, 1991; Buyuksarac *et al.*, 2005).

Outcropping sedimentary formations are mostly composed of Neogene and Quaternary units (Dincer, 1978; Gorur and Derman, 1978; Derman, 1979; Dellalolu and

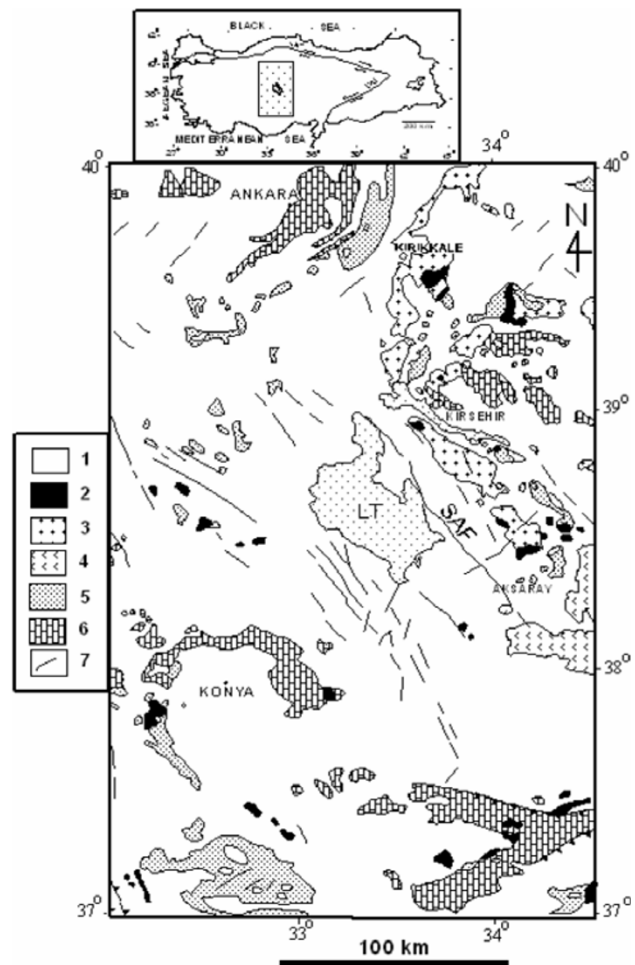


Fig. 2. Geological map of the study area. Modified from Ates *et al.* (2005). Abbreviations: 1, Sedimentary cover; 2, mafic-ultramafic rocks; 3, granitoid; 4, volcanic rocks; 5, ophiolitic rocks; 6, metamorphic rocks; 7, faults; SAF, Sereflikochisar-Aksaray Fault.

Aksu, 1984; Dellalolu, 1991). The older sedimentary units outcrop around the eastern and western boundaries of the Tuzgolu Basin in very smaller areas than the acreage of ophiolitic and volcanic rocks. The most obvious structural unit on the surface (Fig. 2) is the right lateral strike-slip, the Sereflikochisar-Aksaray Fault (SAF).

The general stratigraphic columnar section is illustrated in Fig. 3. The sedimentary deposition of the Tuzgolu Basin unconformably overlies the metamorphic basements of the Kırşehir Block and Kutahya-Bolkardagi Unit of the Menderes-Taurus Platform. These metamorphic units are exposed along the eastern and western margins of Tuzgolu Basin and are composed of metasedimentary rocks that are lithologically similar to each other. Sedimentary deposition in the research area starts with terrestrial redbeds and conglomerates as the oldest sedimentary rocks (Late Maastrichtian Kartal Formation), while turbidites and other deep sedimentary units, named the Haymana Formation, are deposited in deeper parts of the basin. These equivalent units in age grade in an upward direction into the relatively shallow-marine turbidites mainly composed of shales, siltstones, sandstones and reefoidal limestones that developed on the paleo-highs during the Paleocene. The

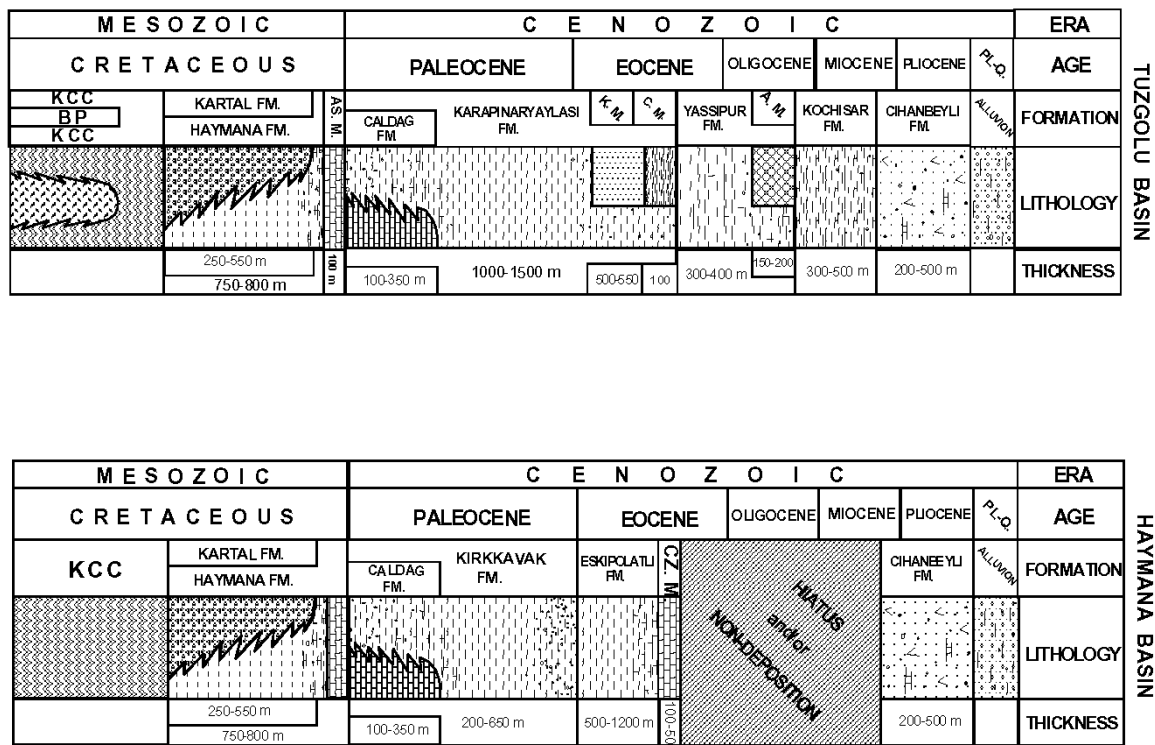


Fig. 3. Generalized stratigraphic columnar section of the study area. PL-Q. Plio-Quaternary Unit; AM, Akbogaz Member; CM, Cavuskalesi Member; KM, Karamollausagi Member; CZM, Cayraz Member; ASM, Asmayaylasi Member; BP, Baranadag Pluton; KCC, Kirsehir Crystalline Complex.

reefoidal limestone is referred to as the Caldag Formation, and the turbidites are named the Kirkkavak Formation (Fig. 3). Along the western margin, Paleocene and Eocene units can be distinguished from each other on the basis of lithological changes. However, it is very difficult to distinguish Eocene units from their Paleocene counterparts; consequently, along the eastern margin they are collectively named the Karapinaryaylasi Formation (Dellaloglu and Aksu, 1984). Along the eastern margin the Eocene units are named the Eskipolatli Formation. The end of the Middle Eocene is the time of collision and merging of all plates and blocks for the assemblage of Anatolides. As a result of this major tectonic gathering, the Tuzgolu Basin shallowed and became a lacustrine environment, giving way to terrestrial, lacustrine and evaporite deposition at the end of Lutetian (Gorur *et al.*, 1998). The sedimentary unit that is the product of this sedimentation period is called the Yassipur Formation. The Eocene and Oligocene contact can be distinguished by an unconformity surface (Fig. 3). The Yassipur Formation is composed of coarse-grained sandstones and a thick evaporite unit (named Akbogaz Member) overlaid by an unconformity. The Oligo-Miocene age Kochisar Formation unconformably overlies all of the Eocene units in the Tuzgolu Basin, while the Haymana Basin was exposed during the Oligo-Miocene; the Yassipur and Kochisar Formations are not observed around this basin. Finally, the Mio-Pliocene-aged Cihanbeyli Formation unconformably overlies all of the older rocks and covers almost all of the study area (Fig. 2). The lithology of this unit consists of conglomerate, sandstone, siltstone, claystone and lacustrine limestones. It also contains volcanic units interbedded with the sedimentary units locally.

3. Topography of the Region and Geophysical Data

3.1 Aeromagnetic data

The topographical map (Fig. 4) reveals that the study area has a smooth and stable topography from which all sorts of geophysical data can be acquired conveniently. However, it is more practical to collect the data using an aeronautical service given the size of the study area. The gravity and aeromagnetic data used in this study were obtained from the General Directorate of Mineral Research and Exploration (MTA) of Turkey. The aeromagnetic data were collected by means of an aeronautical survey carried out at an altitude of 600 m (2000 ft). The total components of the geomagnetic field were measured along the N-S trending profiles, and the measured values were subsequently reduced to October 1982 with daily variation and direction error corrections. The "International Geomagnetic Reference Field-IGRF" values were calculated using a programme from the Baldwin and Langel (1993). The residual magnetic anomaly map after removing IGRF values is given in Fig. 5. The most obvious feature on this map (Fig. 5) is the existence of a broad anomaly crossing the study area in the NW to SE direction; this was named for the first time by Aydemir (2005) as the Suluklu-Cihanbeyli-Goloren Anomaly. Another magnetic anomaly is observed around the northernmost corner of Lake Tuzgolu; this is named the Deliler Anomaly. It is thought that the volcanic mass beneath the surface creates this anomaly. There are some other obvious anomalies in Fig. 5, such as the anomaly to the south of Konya studied by Ates and Kearey (2000), the other one to the east of Aksaray studied by Buyuksarac *et al.* (2005) and the last one to the north of Kaman. However, their lo-

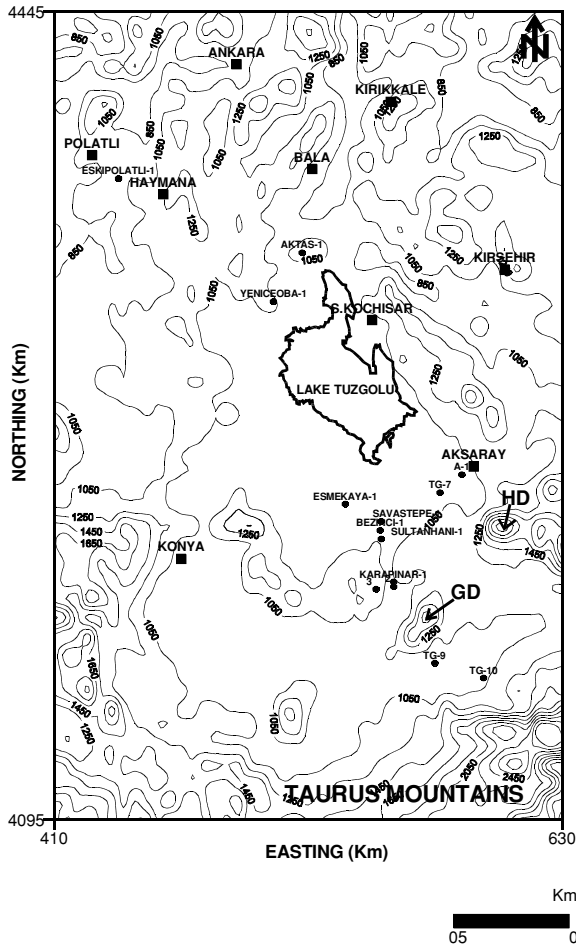


Fig. 4. Topographical map of the study area: HD, Mount Hasandagi; GD, Goloren High. Contour interval is 200 m. Borehole abbreviations: TG-9, Tuzgolu-9; TG-10, Tuzgolu-10; A-1, Aksaray-1; 2, Karapinar-2; 3, Karapinar-3.

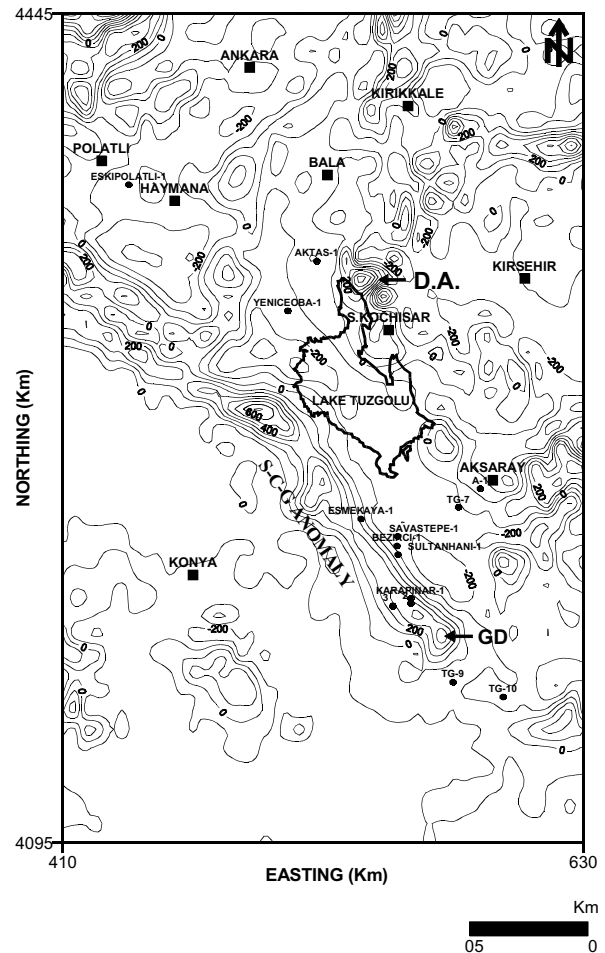


Fig. 5. Residual aeromagnetic anomaly map of the study area. GD, Goloren High; DA, Deliler anomaly; S-C-G ANOMALY, Suluklu-Cihanbeyli-Goloren Anomaly; Contour interval, 100 nT. Borehole abbreviations: TG-9, Tuzgolu-9; TG-10, Tuzgolu-10; A-1, Aksaray-1; 2, Karapinar-2; 3, Karapinar-3.

cations are beyond the boundaries of the Tuzgolu and Haymana Basins and as such are not the subject of this study.

3.2 Gravity data

The collected gravity data were tied to the Potsdam (981260.00 mGal) base value. All necessary corrections were applied to the gravity data, such as latitude, free-air, Bouguer correction (Bouguer correction was carried out for a density of 2.40 g/cm^3), topographical and tidal corrections. The gravity and aeromagnetic data were then both gridded at 2.5-km grid intervals. The gravity anomaly map is given in Fig. 6 with city centres and the boundary of Lake Tuzgolu.

Some important results from the study of Aydemir and Ates (2005) are as follows. (1) The southeastern part of the Tuzgolu Basin is sometimes named the Ulukisla Basin in previous studies. According to the gravity and aeromagnetic anomaly maps and their upward continuation maps (Aydemir and Ates, 2005), there is no dividing structure or anomaly to separate the major basin into two basins. Based on these maps, only one name, the Tuzgolu Basin, is used for the area under study. The partition of the whole basin is only valid geographically. (2) The Haymana Basin is located to the east of Haymana city centre, extending in the N-NE to S-SW direction. This is contrary to assumptions

made in earlier studies in which the basin was thought to be located around the centre of Haymana city and to the west. The other basin, called the Kirikkale Basin, is separated from the Haymana Basin by a saddle-shaped feature around Bala and extends in a line parallel to both the Haymana and Kirikkale basins. This basin is not as clearly evident as the other basins. (3) The third important observation made by Aydemir and Ates (2005) is the existence of a channel-shaped basin to the west of Lake Tuzgolu that connects the Tuzgolu and Haymana Basins. This basin, now called the Tersakan Basin, was first given this name by Aydemir (2005). The Suluklu-Cihanbeyli-Goloren Magnetic Anomaly extends to the west of these basins as a boundary.

3.3 Seismic data

There are approximately 5500 km of 2-D seismic data, most of which were acquired by the Turkish Petroleum Corporation (TPAO) in the Tuzgolu and other basins. The older seismic lines with a low coverage (12-fold) were shot using dynamite and geoflex as energy sources. After 1990, the modern and sophisticated recording instruments with the vibroseis technology were used to acquire 60-fold seismic data. In addition to the acquisition of data, more recent and innovative data processing techniques were applied to

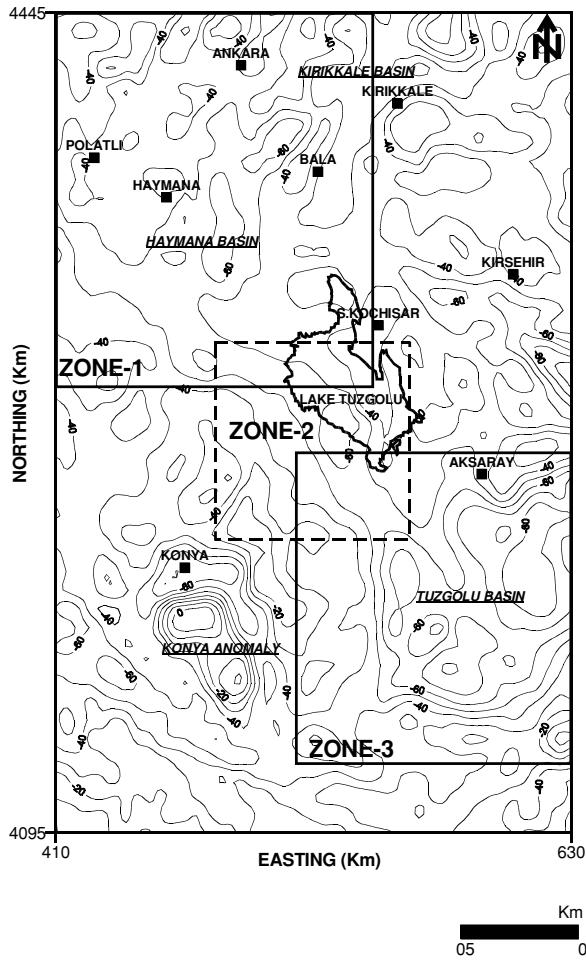


Fig. 6. Gravity anomaly map of the study area. Zone 1 to 3 shows investigated parts in detailed. Contour interval: 10 mGal.

data in order to improve the quality of the seismic lines. Unfortunately, the quality of the seismic lines is still too inadequate to be used as the sole source for accurate interpretation of the seismic. Therefore, we integrated all of the available geophysical data in this study in order to obtain accurate results on the deep structure of the basins. Seismic sections used in this study were obtained from the General Directorate of Petroleum Affairs (GDPA).

3.4 Well data

These basins have been subjected to hydrocarbon exploration activities since the end of 1950s. A total of 30 (including seven re-entries) wells have been drilled to date in the study area, mostly by the TPAO; some of these were drilled for stratigraphic purposes. As a result of the limited amount of geologic data obtained from the isolated outcrops, all of the well data were used to delineate the geological history, stratigraphy and tectonics of the basin together with the surface geology. The composite logs of wells used in this study were also provided by the GDPA.

4. Integration of 3-D Gravity Modelling and Seismic Interpretations

Gravity anomalies were modelled 3-D using a computer program developed by Cordell and Henderson (1968). The 3-D automatic modelling can be calculated for a causative

Table 1. Average interval velocities of sedimentary formations.

Formation	Average thickness (m)	Average velocity (m s^{-1})
Kochisar Formation	802	3042
Eskipolatli Formation	518	4260
Kirkkavak Formation	814	4091
Haymana Formation	1113	4488
Kartal Formation	1080	4518
Average		4080

body assumed to be flat-topped or flat-bottomed. The models are constructed based on the assumption that they are flat topped as the causative bodies in the study area are syncline-shaped. Density contrast is the most important parameter for the construction of models. Densities to be used for the calculation of density contrast between the basement and sedimentary units were obtained from the literature (Telford *et al.*, 1990) and from the velocity versus density graphics produced by Ludwig *et al.* (1970) using the average composition of interval velocities obtained from the sonic logs. Table 1 shows average interval velocities of sedimentary formations in the study area obtained from the sonic logs. The average value of formation velocities is around 4080 m s^{-1} . The corresponding density value of this velocity on the chart proposed by Ludwig *et al.* (1970) takes place between 2.35 and 2.40 g cm^{-3} . These density values are consistent with the densities of shales and sandstones obtained from the literature (Telford *et al.*, 1990). When the limestones deposited on isolated paleo-highs and evaporites are included, the sedimentary basin fill is mainly composed of turbiditic units, with shales and sandstones the most dominant forms, so that 2.40 g cm^{-3} can be accepted as a descriptive value for the sedimentary basin fill. Furthermore, the basement of the basin is composed of schists, marbles with intensive schistosity and graywackes. Although, there are two different metamorphic units constituting the basement, the similarity of their lithologies and geophysical responses suggests that they can be accepted as a single basement. The densities of these metamorphic units are given as being about 2.64 – 2.65 gr cm^{-3} by Telford *et al.* (1990). In this respect, 0.25 g cm^{-3} can be taken as the density difference between the sedimentary fill and basement. Consequently, the Haymana, Tersakan and Tuzgolu Basins were first modelled in accordance with this density contrast, and then the depth values of 3-D model maps were correlated by the available well data and depth values of interpreted seismic sections. The well data were taken into consideration when interpreting the seismic sections and were applied onto the three-dimensional model maps. The horizon representing the basement was followed in order to check the 3-D models and to compare the geometries and depth values of the basement observed. Following the interpretation of the seismic sections, RMS velocities of each section were ordered from shallow to deeper velocities. The depth of followed horizon (basement) was then calculated at irregularly selected shot points. The “time-velocity-depth” table (Table 2) was the result of this procedure, and depth results were correlated with the 3-D model maps. In comparison to the depth results, a good consistency was ob-

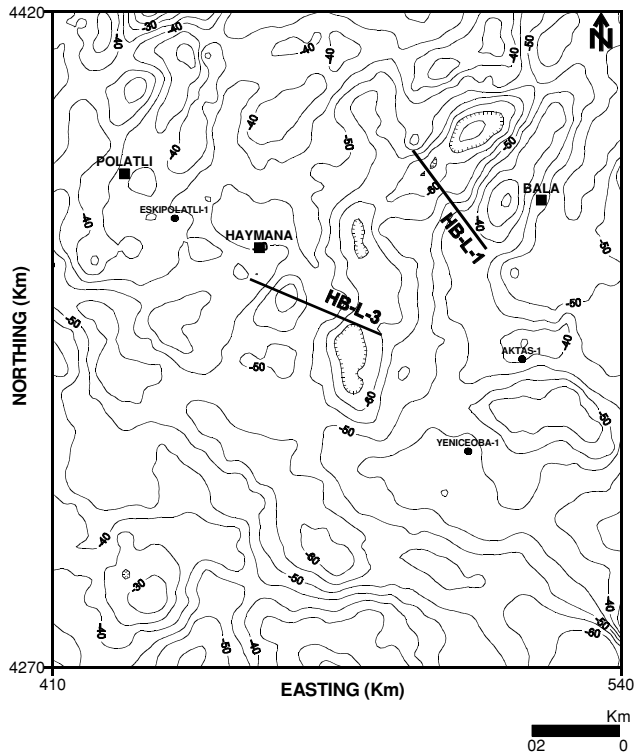


Fig. 7. Gravity anomaly map of Haymana Basin. Contour interval: 5 mGal. Lows are cross-hatched.

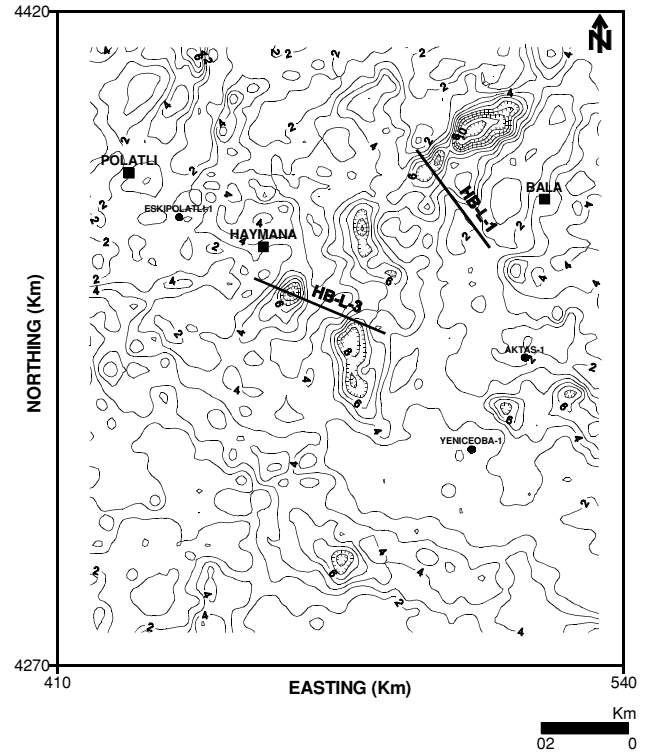


Fig. 8. Three-dimensional gravity model of the Haymana Basin. Contour interval: 1 km. Depths more than 7 km are cross-hatched.

tained. The following subsections will examine the Haymana, Tersakan and Tuzgolu Basins in detail.

4.1 Haymana Basin

The gravity anomaly map of the Haymana Basin (Zone 1 in Fig. 6) is given in Fig. 7. The important towns such as Haymana, Polatli, Bala and well locations together with two seismic lines are also shown in this figure. The 3-D model map of this area is given in Fig. 8. There are four different, obviously deeper segments in the basin. Two of these are located to the south, among Haymana city and the Yeniceoba-1 and Aktas-1 wells; one is located in the middle of the depression zone—20–25 km east of Haymana city centre; the fourth is located to the north, 25 km away from the centre of Bala city. The deepest parts of the southern depressions and the depression in the middle are 8 km in depth, while the depression to the north reaches down to 11 km. The seismic line HB-L-1 (Fig. 9) crosses the southern edge of the depression area in the north where the deepest contours are between 7 and 8 km at depth and verifies the depth of the basement. The “Time-Velocity-Depth” table is given in Table 2. RMS velocities are generally lower than 4080 m s^{-1} , which is the average of the interval velocities for the whole sedimentological section and used to determine the density contrast for modelling. It is 3900 m s^{-1} at the shot point (SP) 750 according to the deepest part of basement in the section and the cross-point of the section on the model map (Fig. 8). The calculated depth for this SP is 6367 m, which verifies the model map where the depth is expected to be between 6000 and 7000 m. Similar results and good consistency with the model map were obtained at other SPs. The other seismic line, HB-

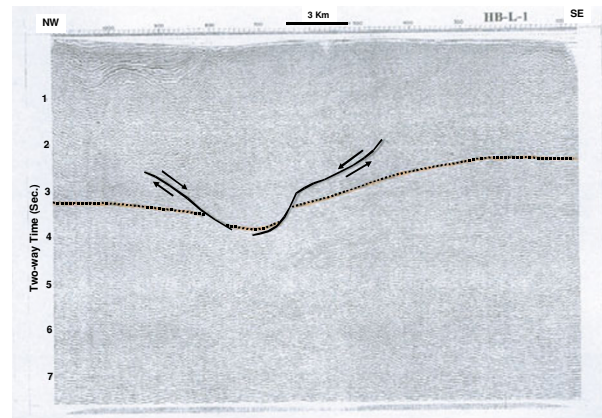


Fig. 9. Seismic Line HB-L-1 crosses the northern depression of the Haymana Basin. Vertical axis represents two-way travel time (TWT) in seconds.

L-3 (Fig. 10), extends in a NW-SE direction, crossing the centre of the depression area to the south, closer to the centre of Haymana city. SP: 320 is located at the middle of the depression, both on the seismic section and the model map. The calculated depth at this SP is 7800 m, which is very close to the 8000 m observed on the model map. The other SPs also have depth values that are consistent with those of the model map. However, this consistency can not be proved by the well data because none of the three wells drilled in this basin penetrated the basement, although they were abandoned in formations overlying the basement.

4.2 Tersakan Basin

The gravity anomaly map of the Tersakan Basin (Zone 2 in Fig. 6) is given in Fig. 11. Well locations together with

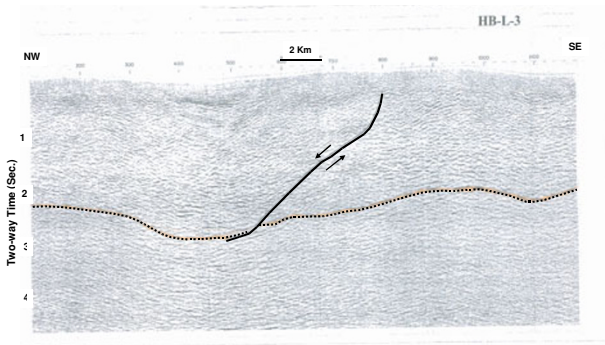


Fig. 10. Seismic Line HB-L-3 crosses the southern depression close to the centre of Haymana city. Vertical axis represents two-way travel time (TWT) in seconds.

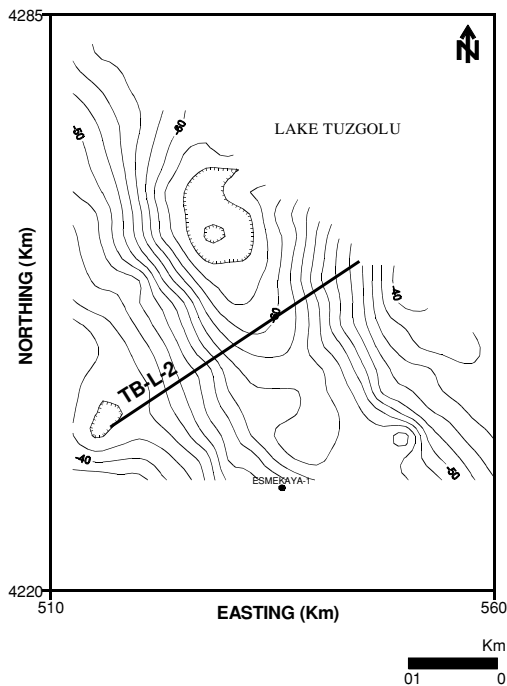


Fig. 11. Gravity anomaly map of Tersakan Basin. Contour interval: 2 mGal. Lows are cross-hatched.

a characteristic seismic line crossing this channel-shaped basin in the middle are also shown in this figure. This channel-shaped basin connects the Haymana and Tuzgolu Basins. The 3-D model of this area is given in Fig. 12. There is only one depression observed in this basin, the deepest part of which reaches down to 5.5 km. The seismic line TB-L-2 (Fig. 13) crosses the depression area in the middle where the deepest contours are between 3.5 and 4 km, thereby verifying the depth of basement when the “Time-Velocity-Depth” table (given in Table 2) is examined. This line has a depth of 1450 m at SP: 420 in the southwestern edge, and it has almost an exact depth consistency at SP: 700, which represents the deepest part at a depth of 3920 m. The seismic line is almost tangent at this SP to the 4-km depth contour of the model map (Fig. 12). The northeastern part of the line is also consistent with that of the model map. SP: 980 is located in between the contours of 2.5 and 3 km where the depth value decreases down to 2900 m (Table 2).

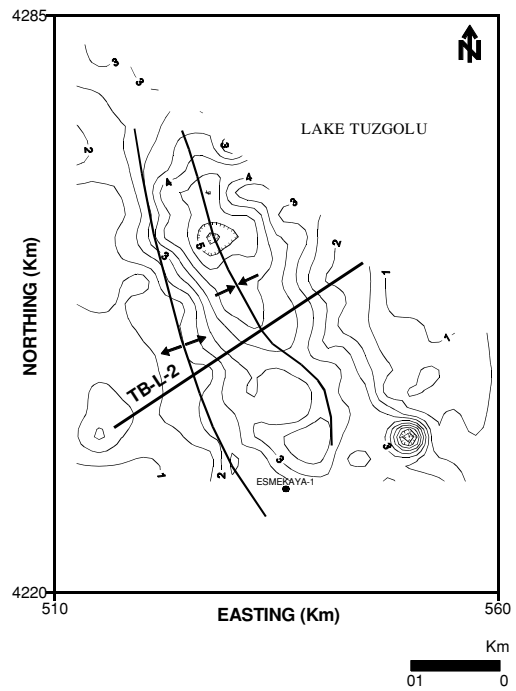


Fig. 12. Three-dimensional gravity model of the Tersakan Basin. Contour interval: 0.5 km. Depths more than 5 km are cross-hatched.

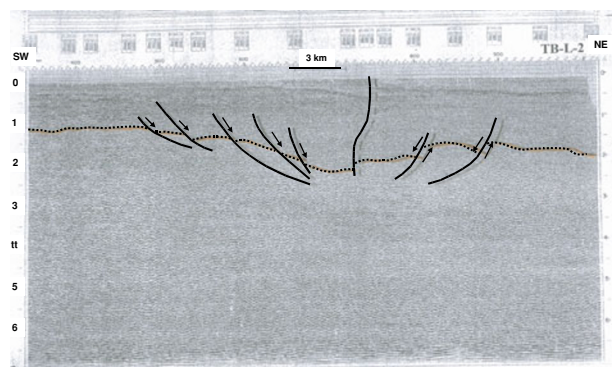


Fig. 13. Seismic Line TB-L-2 shows the stepwise faulting mechanism of the Tersakan Basin. Vertical axis represents two-way travel time (TWT) in seconds.

4.3 Tuzgolu Basin

The gravity anomaly map of the Tuzgolu Basin (Zone 3 in Fig. 6) is given in Fig. 14. The city centre of Aksaray and the well locations together with four seismic lines are also shown in this figure. The 3-D model map of this area is given in Fig. 15. This basin is the largest basin in Central Anatolia, and most of the exploration activities in Central Anatolian basins were carried out in this basin. Partially because these exploration activities were carried out at different times by different companies, the results of the different geological and geophysical methods were never integrated. There are three main depression zones in this basin: (1) the Southern Aksaray Depression, (2) the Eregli Depression and (3) The Sultanhani Depression. Due to the high level of disorganisation of these earlier exploration activities, the latter were concentrated only in the Sultanhani Depression, with insufficient data on the Eregli Depres-

Table 2. Time-velocity-depth table of seismic sections in the study area.

Seismic line	SP	Time (s)	Velocity (m s ⁻¹)	Depth (m)
HB-L-1	175	2200	3043	3347
	340	2500	3096	3870
	455	2800	3148	4407
	655	3500	3223	5640
	690	3700	3244	6001
	750	3900	3265	6367
	900	3400	3212	5460
HB-L-3	120	2200	5330	5863
	320	2700	5777	7799
	400, 720	2396	5517	6609
TB-L-2	880, 1100	1976	4874	4816
	350	1200	2720	1632
EB-L-3	420	1100	2629	1446
	580	1500	2970	2228
	630, 900	1800	3154	2839
	700	2300	3410	3922
	830	1900	3211	3050
	120, 420	2600	4150	5395
	180	2900	4319	6263
TG-NL-1	270	3000	4375	6563
	520	2100	3887	4081
	620, 800	2200	3939	4333
	720	2400	4045	4854
	110, 200	2250	3635	4089
	320	2375	3900	4631
	550	2800	4236	5930
	920	3600	4513	8123
	1330	3000	4289	6434
	1520	2700	4210	5684
TG-WL-4	1740	3300	4369	7209
	540	2500	3304	4130
	640	2600	3351	4356
	720	2900	3490	5061
TG-WL-6	940	3200	3629	5806
	140	3600	3753	6755
	240	2500	3080	3850
	420	2300	2973	3419

sion. The Southern Aksaray Depression is the largest unexplored depression, and it consists of three sub-depressions. The possible reason for this lack of any exploration activity could be the presence of younger volcanic activity to the east, resulting in volcanic cover of this area. The Southern Aksaray Depression is separated from the Sultanhani Depression by a tectonic high named the Southern Tuzgolu High. However, there is no obvious separator, either volcanic or tectonic, between the Southern Aksaray and Eregli Depressions. There is a young volcanic eruption centre—the Goloren Mountain—which is located on the southeastern edge of the Suluklu-Cihanbeyli-Goloren magnetic anomaly; this eruption separates the Sultanhani and Eregli Depressions.

The deepest sub-depression of the Southern Aksaray Depression is located about 30–35 km southeast of Aksaray, and its deepest centre reaches down to a depth 12–13 km. This sub-depression is shown as the Southern Aksaray Sub-depression-1 (SAS-1) in the 3-D model map (Fig. 15). The

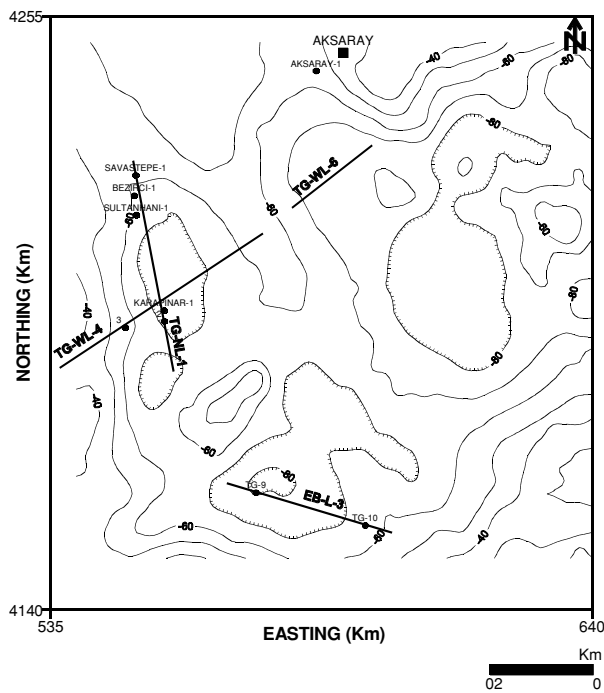


Fig. 14. Gravity anomaly map of Tuzgolu Basin. Contour interval: 10 mGal. Lows are cross-hatched. Borehole abbreviations: TG-9, Tuzgolu-9; TG-10, Tuzgolu-10; 2, Karapinar-2; 3, Karapinar-3.

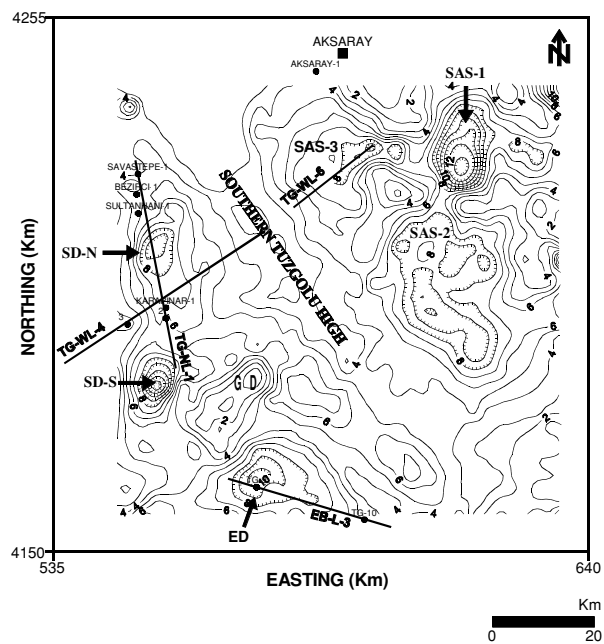


Fig. 15. Three-dimensional gravity model of the Tuzgolu Basin. Contour interval: 1 km. Lows from 8 to 13 km are cross-hatched. SAS-1, Southern Aksaray Sub-depression-1; SAS-2, Southern Aksaray Sub-depression-2; SAS-3, Southern Aksaray Sub-depression-3; SD-N, Sultanhani Depression-North; SD-S, Sultanhani Depression-South. Borehole abbreviations: TG-9, Tuzgolu-9; TG-10, Tuzgolu-10; 2, Karapinar-2; 3, Karapinar-3.

sub-depression to the far south, represented by the 8-km contour, reaches down to a depth of 9 km and is named the SAS-2. The third sub-depression, shown as SAS-3, is located to the west of SAS-1 and about 20–25 km away from Aksaray. Its deepest part is also represented by an 8-

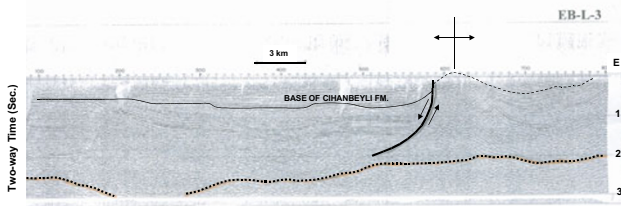


Fig. 16. Seismic Line EB-L-3 crosses the Eregli Depression. The base of the Cihanbeyli Formation represents an unconformity surface. Vertical axis represents two-way travel time (TWT) in seconds.

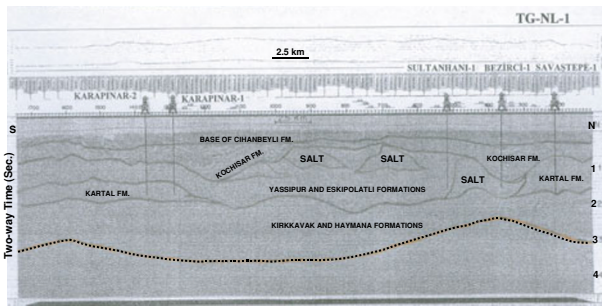


Fig. 17. Seismic Line TG-NL-1 crosses the Sultanhani Depression-North (SD-N). The line crosses through five wells, thereby enabling the well control. The section also shows some possible salt structures that the salt diapire on the right was penetrated by the Bezirci-1 well. Vertical axis represents two-way travel time (TWT) in seconds.

km contour. The Southern Aksaray Depression as a whole covers an area of at least $50 \times 10 \text{ km}^2$ despite having some higher areas in and around these sub-depressions. Unfortunately, this modelling study is the only available information on the subsurface of this depression because there is no seismic and well data for this area.

The Eregli Depression located to the north of Taurus Mountains (Fig. 4) is yet another major depression area in

the Tuzgolu Basin. The maximum depth of this depression is about 10 km at the location of the TG-9 well. The total acreage is about $15 \times 10 \text{ km}^2$. An insufficient amount of seismic data were acquired at the beginning of the 1970s, and two shallow wells were drilled for stratigraphic analysis of the sedimentary deposition. Seismic line EB-L-3 (Fig. 16) crosses the deepest zone of the depression area where the depth contours are between 9 and 10 km. This depth can be verified as the depth of basement when the “Time-Velocity-Depth” table (given in Table 2) is examined. Although the record length is longer, the seismic section was processed down to 3 seconds, which is insufficient to interpret the deeper part of the depression. However, the eastern part of the section can be followed to enable a comparison with the 3-D model map. The calculated depth at the SP: 800 located on the eastern end of the line is 4300 m, which is consistent with the 3-D model. The basement horizon can not be followed after SP: 420, which has a 5400 m depth value. Because the purpose of drilling the two shallow wells (TG-9 and TG-10) was to analyse the stratigraphy, the consistency can not be proved by the well data.

The most explored section of the Tuzgolu Basin is the N-S trending Sultanhani Depression. Most of the seismic data were acquired in this depression, and the deeper hydrocarbon exploration wells were drilled on the margin of this depression, which is also the margin of the Tuzgolu Basin. This basin is separated from the other major depressions by the Southern Tuzgolu High to the east and the Goloren Mountain to the southeast. It is composed of two sub-depressions: the explored one to the north, named the Sultanhani Depression-North (SD-N), and the unexplored one to the south, named SD-S. The deepest part of the depression was observed in the SD-S, about 12 km. Unfortunately, this is not supported by the model due to the lack of seismic and well data. However, the SD-N depression becomes less deep, down to only 8–9 km. The seismic line TG-NL-1

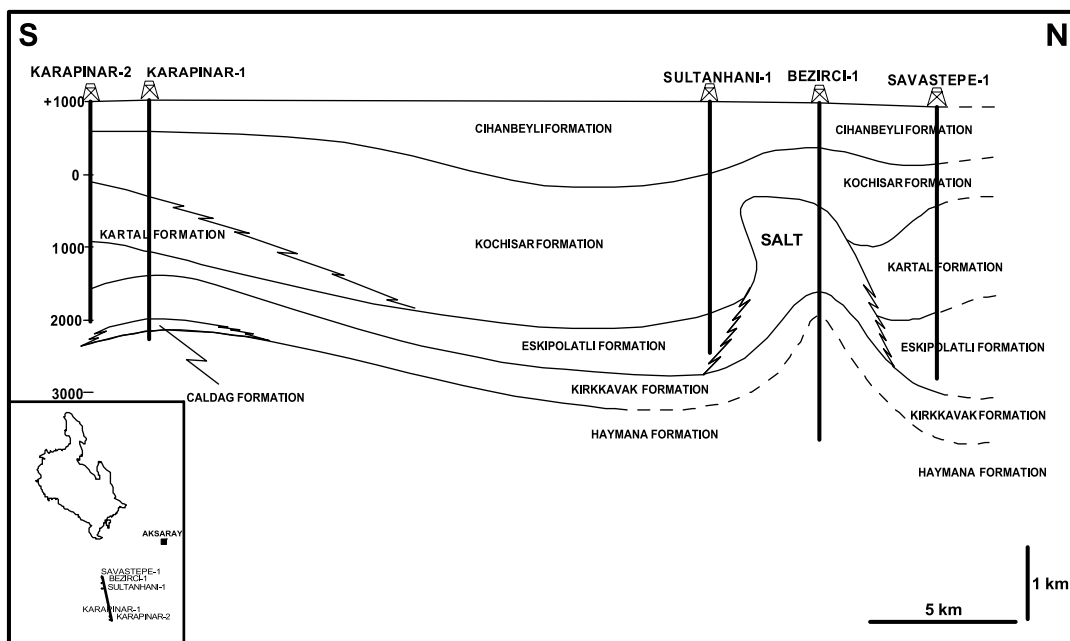


Fig. 18. Geological cross-section crossing of the Karapinar-2, Karapinar-1, Sultanhani-1, Bezirci-1 and Savastepe-1 wells.

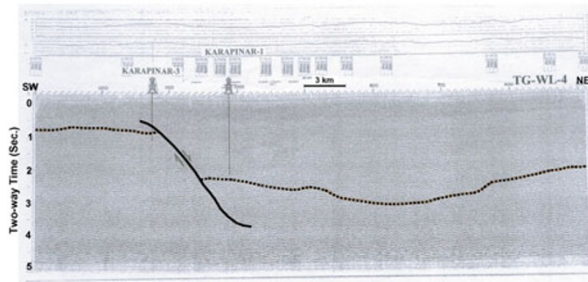


Fig. 19. Seismic Line TG-WL-4 crosses the Sultanhani Depression-North (SD-N). The line crosses through two wells and shows a possible shale diapire to the east of the Karapinar-1 well. The Karapinar-3 well was penetrated the basement at the depth of 1315 m and abandoned in basement at the Total Depth (TD) of 1570 m. Vertical axis represents two-way travel time (TWT) in seconds.

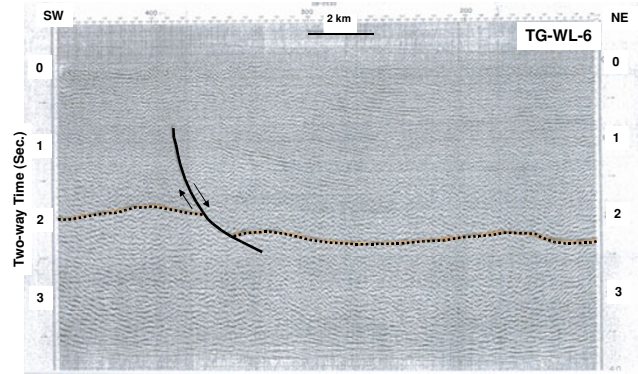


Fig. 20. Seismic Line TG-WL-6 shows the deepening through the Southern Aksaray Depression-3 (SAS-3). Vertical axis represents two-way travel time (TWT) in seconds.

(Fig. 17) extends from south to north, crossing this depression in the middle and along many exploration wells. The calculated depth on the southern end at SP: 1330 is about 6450 m. This SP is located in between the 6- to 7-km depth contours in the map (Fig. 15). The deepest part of the selected horizon on the seismic section coincides to SP: 920, with a calculated depth of 8123 m; this part is found within the closed contour of 8 km. Other calculated depths at different SPs are also consistent with the 3-D model and can be proven by the well data. This seismic section, TG-NL-1, passes through five exploration wells. Although none of five wells penetrated the basement, some were abandoned in formations just above the basement. It can be deduced from their total depths (TDs) that they are very close to the basement depth in the model maps. In order to verify the representability of seismic section, a geological cross-section (Fig. 18) was prepared based only on the well results, without taking the seismic section into consideration. The similarity between the cross section and the interpretation of the seismic section is very obvious. The seismic line TG-WL-4 is an E-W trending line that crosses the southern edge of the SD-N depression (Fig. 19). This line is also consistently representative of the model map, but RMS velocities are lower than the average sedimentary fill velocity (4080 m s^{-1}) so that calculated depth values are 275–300 m lower than the 3-D model shown in Fig. 15. This inconsistency of depth values are also observed in the well data. The considered line extends to the Karapinar-3 and Karapinar-1 wells. SP: 1125 coincides with the Karapinar-3 well that penetrated the metamorphic basement at a depth of 1315 m. The calculated depth at the SP: 1120 is about 1043 m, and the difference is 272 m. This discrepancy is also valid for the Karapinar-1 well and for the intersection point with the line TG-NL-1. The depth values can be calibrated by adding up the $380\text{--}400 \text{ m s}^{-1}$ velocity difference to all RMS velocities so that a good consistency can be obtained. The seismic line TG-WL-6 is the last example which indicates that the basin deepens toward the SAS-3 to the east (Fig. 20).

5. Conclusions

The largest and most important basin in the Central Anatolia is the Tuzgolü Basin, which is connected to the Hay-

mana Basin by means of a small channel-shaped basin named the Tersakan Basin. The Tuzgolü Basin and other related basins have smooth and stable surface conditions. Thus, the topography does not reflect the complex subsurface geology and severe tectonics buried beneath the younger sedimentary cover. Older sedimentary units can be observed around the eastern and western boundaries of the Tuzgolü Basin in limited, small areas. The metamorphic units of the Kirsehir Block and Kutahya-Bolkardagi Metamorphic unit overlaid by the sedimentary deposition are also exposed along the eastern and western margins of the Tuzgolü Basin. Both of these units are composed of metasedimentary rocks that are lithologically similar, and their geophysical responses are almost the same. For this reason, they may be accepted as a single basement unit for geophysical investigations. The quality of the seismic sections shot in the study area is poor. This difficulty was overcome by integrating all available geophysical data with each other and with the geological data as well.

Gravity anomalies of the Haymana, Tersakan and Tuzgolü Basins were separately modelled 3-D using a computer programme developed by Cordell and Henderson (1968). The density of 2.40 gr cm^{-3} was accepted as being a representative value for the sedimentary basin fill, and 2.65 gr cm^{-3} was accepted as representative value for the metamorphic basement of the study area. The basin modelling was based on the density contrast between the basement and sedimentary units given above. Depth values of 3-D model maps were subsequently correlated by available well data and by depth values obtained using RMS velocities of the interpreted seismic sections. In comparison to the depth results of 3-D model maps, a good consistency was obtained with the well data and depths from the seismic data for the three basins.

According to the modelling, the deeper parts of the Haymana Basin are located to the east of the centre of Haymana city, which is contrary to the assumptions of earlier studies. These deeper segments of the basin have a maximum depth of 8 km except in the depression to the north (Fig. 8). The northern depression, which is located 25 km northwest of the centre of Bala city, has a maximum depth of 10 km (Fig. 8). The channel-shaped Tersakan Basin (con-

necting Haymana and Tuzgolu Basins) lies to the west of Lake Tuzgolu. The deepest part of this basin is approximately 5.5 km (Fig. 12). Finally, the Tuzgolu Basin, the largest in Central Anatolia, has three major depressions. The first is the Southern Aksaray Depression, which is covered by younger volcanic rocks. It has an average depth of 8 km in its two sub-depressions (SAS-2 and SAS-3), while the deepest sub-depression, located 30–35 km southeast of the centre of Aksaray city (SAS-1), is approximately 12–13 km in depth. The Southern Aksaray Depression (composed of three sub-depressions) covers an area of 500 km², and this important segment of the Tuzgolu Basin is an unexplored area. The Southern Aksaray Depression with its sub-depressions can be considered to be a potential hydrocarbon generation zone. Thus, future exploration activities should be carried out on the prospects located around this area. Gorur *et al.* (1998) pointed out the hydrocarbon potential of the Tuzgolu Basin. The Southern Aksaray Depression is separated from the Sultanhani Depression by the Southern Tuzgolu High. The second major depression is the Eregli Depression (ED) to the south, which covers an area of 150 km². The deepest part is approximately 9–10 km in depth (Fig. 15). The third major depression is the western segment of the Tuzgolu Basin and is named the Sultanhani Depression; most of the previous exploration activities were carried out in this segment. This depression is composed of two sub-depressions: (1) the deepest part of the depression is located to the south (SD-S), approximately at a depth of 12 km, but this depth value is not yet proven due to lack of seismic or well data; (2) the northern sub-depression (SD-N), including almost all of the previous exploration data, has a maximum depth of 9 km (Fig. 15), but contrary to the southern sub-depression, the 3-D model map has been consistently verified by the seismic and well data in this sub-depression.

Acknowledgments. We would like to express our sincere thanks to the Mineral Research and Exploration Institute of Turkey for the use of gravity and magnetic data. Seismic sections and well composite logs were provided for a TUBITAK Project (Project No: YDABCAG-118) by the General Directory of Petroleum Affairs (GDPA). The authors would like to thank Mr. Serdar Demiralın for reading and criticising the manuscript before submission. Financial support was also provided by an Ankara University, Scientific Research Project (Project Code: 20010705050). We also thank Dr. Naoshi Hirata and an anonymous referee for their constructive critical review of the manuscript.

References

- Ates, A., Possibility of deep gabbroic rocks, east of Tuz Lake, Central Turkey, interpreted from aeromagnetic data, *Journal of the Balkan Geophysical Society*, **2**, 15–29, 1999.
- Ates, A. and P. Kearey, Interpretation of gravity and aeromagnetic anomalies of the Konya Region, South Central Turkey, *Journal of the Balkan Geophysical Society*, **3**, 37–44, 2000.
- Ates, A., F. Bilim, and A. Buyuksarac, Curie Point Depth Investigation of Central Anatolia, Turkey, *Pure and Applied Geophysics*, **162**, 357–371, 2005.
- Aydemir, A., Investigation of structural geology and hydrocarbon potential of the Tuzgolu Basin and surrounding area by using geophysical methods, Ph.D. Thesis, Ankara University, Turkey (unpubl.), 2005 (in Turkish with English abstract).
- Aydemir, A. and A. Ates, Preliminary evaluation of Central Anatolian basins in Turkey using the gravity and magnetic data, *Journal of the Balkan Geophysical Society*, **8**, 7–19, 2005.
- Baldwin, R. T. and R. Langel, Tables and maps of the DGRF 1985 and IGRF 1990, International Union of Geodesy and Geophysics Association of Geomagnetism and Aeronomy, *IAGA Bulletin*, **54**, 158, 1993.
- Buyuksarac, A., D. Jordanova, A. Ates, and V. Karloukovski, Interpretation of the gravity and magnetic anomalies of the Cappadocia Region, Central Turkey, *Pure and Applied Geophysics*, **162**, 2197–2213, 2005.
- Cemen, I., C. Goncuoglu, and K. Dirik, Structural Evolution of the Tuzgolu Basin Central Anatolia, Turkey, *Journal of Geology*, **107**, 693–706, 1999.
- Cordell, L. and R. G. Henderson, Iterative three-dimensional solution of gravity anomaly data using a digital computer, *Geophysics*, **33**, 596–601, 1968.
- Dellaloglu, A. A., Ankara-Temelli-Haymana-Kulu-Kirikkale Arasındaki Alaninin Jeolojisi ve Petrol Olanaklari, TPAO Report No: 3006 (unpubl.), 1991 (in Turkish).
- Dellaloglu, A. and R. Aksu, Kulu-Sereflikochisar-Aksaray dolayinin jeolojisi ve petrol olanaklari, TPAO Report No: 2020 (unpubl.), 1984 (in Turkish).
- Derman, A. S., Tuz Golu Dogu ve Kuzeyinin Jeolojisi, TPAO Report No: 1512 (unpubl.), 1979 (in Turkish).
- Dincer, A., Haymana-Kulu Yoresinin Jeoloji ve Petrol Olanaklari, TPAO Report No: 1314 (unpubl.), 1978 (in Turkish).
- Gorur, N. and A. S. Derman, Tuzgolu-Haymana Havzasinin Stratigrafik ve Tektonik Analizi, TPAO Report No: 1514 (unpubl.), 1978 (in Turkish).
- Gorur, N., O. Tuysuz, and A. M. C. Sengor, Tectonic evolution of the Central Anatolian Basins, *Int. Geol. Review*, **40**, 831–850, 1998.
- Gursoy, H., J. D. A. Piper, O. Tatar, and L. Mesci, Paleomagnetic study of the Karaman and Karapinar volcanic complexes, Central Turkey: Neotectonic rotation in the south-central sector of the Anatolian Block, *Tectonophysics*, **299**, 191–211, 1998.
- Kadioglu, Y. K., A. Ates, and N. Gulec, Structural interpretation of gabbroic rocks in Agacoren Granitoid, Central Turkey: Field observations and aeromagnetic data, *Geological Magazine*, **135**, 245–254, 1998.
- Ludwig, J. W., J. E. Nafe, and C. L. Drake, Seismic Refractions, in *The Sea*, edited by A. E. Maxwell, John Wiley, New York, 1970.
- McClusky, S., S. Balassanian, A. Barka, C. Demir, S. Ergintav, I. Georgiev, O. Gurkan, M. Hamburger, K. Hurst, H. Kahle, K. Kastens, G. Kekelidze, R. King, V. Kotzev, O. Lenk, S. Mahmoud, A. Mishin, M. Nadariya, A. Ouzounis, D. Paradissis, Y. Peter, M. Prilepin, R. Reilinger, I. Sanli, H. Seeger, A. Tealeb, M. N. Toksoz, and G. Veis, Global positioning system constraints on plate kinematics and dynamics in the Eastern Mediterranean and Caucasus, *J. Geophys. Res.*, **105**, 5695–5719, 2000.
- Rigo de Righi, M. and A. Cortesini, Regional Studies, Central Anatolian Basin-Progress Report I: Turkish Gulf Oil Co., Petrol Isleri Genel Mudurlugu, ANKARA (unpubl.), 1959 (in Turkish).
- Sanver, M. and E. Ponat, Kirsehir ve dolaylarina iliskin paleomanyetik bulgular, Kirsehir Masifi'nin rotasyonu, *Istanbul Yerbilimleri*, **2**, 231–238, 1981.
- Sengor, A. M. C. and Y. Yilmaz, Tethyan Evolution of Turkey: A Plate tectonic approach, *Tectonophysics*, **75**, 181–241, 1981.
- Telford, W. M., L. P. Geldart, and R. E. Sheriff, *Applied Geophysics* (Second Edition), Cambridge University Press, Cambridge, UK, 1990.
- Ugurtas, G., Tuzgolu Havzasinin bir bolununun jeofizik yorumu, Publication of the Mineral Research and Exploration Institute (MTA) of Turkey, **85**, 38–44, 1975 (in Turkish).
- Unalan, G., V. Yuksel, T. Tekeli, O. Gonenc, Z. Seyit, and S. Huseyin, Haymana-Polatli (GB Ankara) Yoresinin Ust Kretase-Alt Tersiyer Stratigrafisi ve Paleocografik Evrimi, *T. J. K. Bulteni*, **19**, 159–176, 1976 (in Turkish).